Materials Science and Engineering B 298 (2023) 116839

Contents lists available at ScienceDirect

Materials Science & Engineering B

journal homepage: www.elsevier.com/locate/mseb

Comparative analysis of crystallographic phase stability of single and poly-crystalline lead nitrate at dynamic shocked conditions

A. Sivakumar [a], P. Eniya [b], S. Sahaya Jude Dhas [c], Lidong Dai [a,*], P. Sivaprakash [d], Raju Suresh Kumar [e], Abdulrahman I. Almansour [e], J. Kalyana Sundar [b], Ikhyun Kim [d], S.A. Martin Britto Dhas [f,*]

[a] Key Laboratory of High-temperature and High-pressure Study of the Earth's Interior, Institute of Geochemistry, Chinese Academy of Sciences, Guiyang, Guizhou 550081, China
[b] Department of Physics, Periyar University, Salem 636011, Tamil Nadu, India
[c] Department of Physics, Kings Engineering College, Sriperumbudur, Chennai, Tamil Nadu 602 117, India
[d] Department of Mechanical Engineering, Keimyung University, Daegu 42601, Republic of Korea
[e] Department of Chemistry, College of Science, King Saud University, P.O. Box 2455, Riyadh 11451, Saudi Arabia
[f] Shock Wave Research Laboratory, Department of Physics, Abdul Kalam Research Center, Sacred Heart College, Tirupattur, Tamil Nadu 635 601, India

ARTICLE INFO

Keywords:
Shock-waves
Single-crystals
Poly-crystals
Structural stability
Structural Engineering

ABSTRACT

In the present work, we report the crystallographic structural stability of the poly-crystalline lead nitrate samples at shocked conditions with which a systematic comparison is made for the previously reported single-crystalline lead nitrate crystal at shocked conditions. X-ray diffractometry (XRD) and Raman spectroscopic measurements have been performed to assess the crystallographic structural stability of poly-crystalline $Pb(NO_3)_2$ samples at shocked conditions and the observed XRD and Raman results disclose that the title poly-crystalline samples retain the original crystallographic structure even at 100 shocked conditions interacting with the shock waves of 2.2 Mach number. But the single crystals of $Pb(NO_3)_2$ undergo crystalline to amorphous phase transition at shocked conditions. Based on the observed results, poly-crystalline samples have higher-structural stability than that of single crystals. The outcome of this work provides glimpses of possible further contributions to crystal engineering for the design of new materials with specific physical and chemical properties.

1. Introduction

Research on the aftermath effect of dynamic shock waves on materials has been reinforced by the revitalized outcomes such that there could be augmented progress with which tremendous growth is likely to be impended thereby future course of actions of probable stable materials might be standardized so as to meet the industrial and scientific requirements of today and tomorrow. On these counts, the impact of dynamic shock waves on crystallographic structural stability analysis of materials is now considered as a prominent research topic in academia as well as the frontier field of science and technology [1–4]. As far as it is known, the outcomes of dynamic shock wave impact of structural properties on bulk single crystals and poly-crystalline materials (micro and nano-crystalline materials) have been reported which have a lot of interesting behaviors. The structural stability of single crystalline materials such as cyclotrimethylene trinitramine (RDX) [5], sapphire ($\alpha = Al_2O_3$) [6], pentaerythritol Tetranitrate [7], copper (Cu) [8] cadmium sulfide (CdS) [9], potassium sulfate (K_2SO_4) [10], sodium sulfate (Na_2SO_4) [11], ammonium dihydrogen phosphate (ADP) [12], potassium dihydrogen phosphate (KDP) [13], glycine phosphite (GPI) [14] copper sulfate pentahydrate ($CuSO_4{\cdot}5H_2O$) [15], and lead nitrate ($PbNO_3$) [16] have been investigated after exposing them to shock waves. Among the listed crystals, some of the crystals undergo significant crystallographic phase transitions such as potassium sulfate [10] and sodium sulfate [11] at shocked conditions. In the case of poly-crystalline type materials (micro-particles) as that of potassium sulfate [17], ammonium dihydrogen phosphate [18], potassium dihydrogen phosphate [19], glycine phosphite [20] copper sulfate pentahydrate [21], magnesium diboride [22], benzophenone [23] have been investigated at shocked conditions and found that there is no crystallographic phase transition occurred, but structural deformations have been noticed. In addition to that, in the case of nano-crystalline materials,

* Corresponding authors.
E-mail addresses: dailidong@vip.gyig.ac.cn (L. Dai), martinbritto@shctpt.edu (S.A. Martin Britto Dhas).

https://doi.org/10.1016/j.mseb.2023.116839
Received 7 July 2023; Accepted 25 August 2023
Available online 9 September 2023

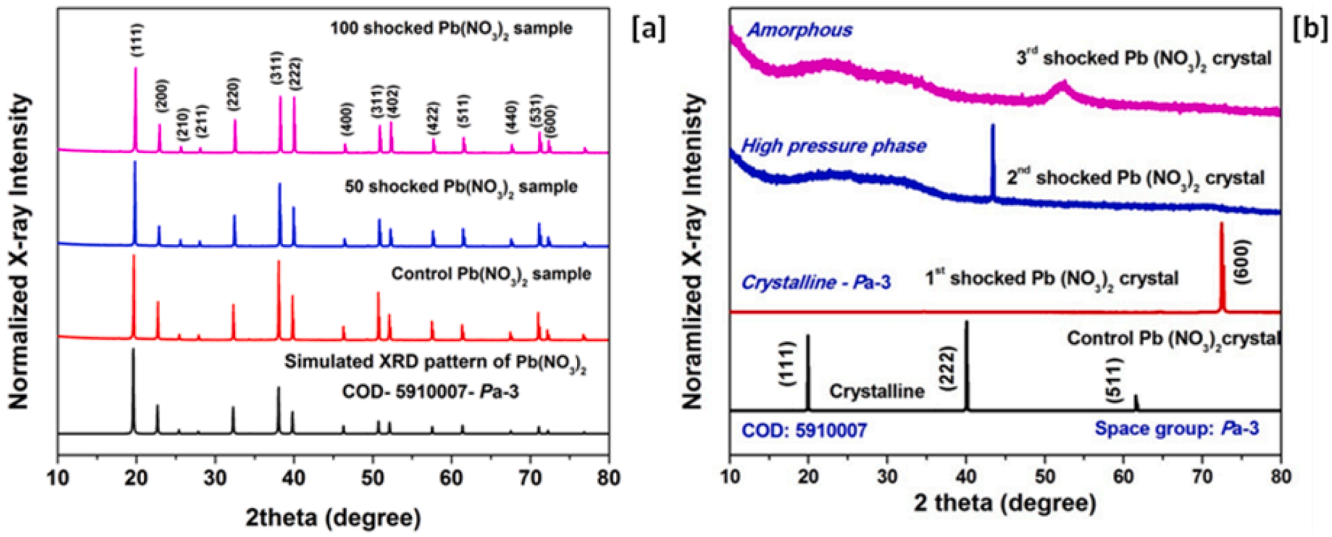

Fig. 1. XRD patterns of the control and shocked lead nitrate samples (a) poly-crystalline (b) Single crystalline $Pb(NO_3)_2$ (Reprint adapted with the permission from Ref [16]).

titanium oxide (TiO_2) [24], zirconium oxide (ZrO_2) [25], and cobalt oxide (Co_3O_4) [26], crystallographic phase transitions have been demonstrated at shocked conditions whereas some of the nano-crystalline materials such as zinc oxide (ZnO) [27], nickel oxide (NiO) [28] cerium oxide [29], molybdenum disulfide (MoS_2) [30], tungsten disulfide (WS_2) [30], molybdenum diselenide ($MoSe_2$) [30] show stable crystal structures at shocked conditions. Based on the above-mentioned literature reports in all possible aspects, the phase transition probability, phase transitions shock pressure and their respective changes in functional properties highly depend on the solid state nature (such as single, poly-crystals and nano materials) of the test samples [5–30].

In general, materials science point of view, poly-crystalline materials have higher structural stability and mechanical stability than that of single crystals for the static pressure and static temperature [31,32]. Gopal Das *et al.* have investigated the thermal stability of single and poly-crystalline α-Al_2O_3 and found that the poly-crystalline materials have higher thermal stability than that of the single crystal [33]. Laurent Mezeix *et al.* have demonstrated the mechanical properties of single and polycrystalline materials and observed that the poly-crystalline materials have slightly higher values of hardness and fracture toughness [34]. The observed profiles of shock resistance of single and polycrystalline materials that have been investigated very well authenticate the above-mentioned concepts [17,21]. But, a thorough understanding of the outcomes of the structural stabilities of single and poly-crystalline materials at harsh environmental conditions such as high-temperature, high-pressure, shock waves and high energy gamma rays is yet to be achieved. In this work, we focus on the structural stability of poly-crystalline material $Pb(NO_3)_2$ at shocked conditions and the obtained results of spectroscopic analyses are compared with the phase stability of $Pb(NO_3)_2$ single crystal at shocked conditions. Based on the previous report, $Pb(NO_3)_2$ single crystal experiences a few significant structural changes at shocked conditions such that the observed shocked phase-profile is *P*a-3 – *P*a-3 – high-pressure phase – amorphous for the 0, 1, 2 and 3rd shocked conditions, respectively [16]. Such kind of interesting results lead to further investigation on its poly-crystalline nature at dynamic shocked conditions.

In this report, we have assessed the crystallographic structural stability of the poly-crystalline $Pb(NO_3)_2$ samples at shocked conditions such that the behavior of shock resistance (crystallographic phase stability) has been analyzed making use of the observed X-ray diffraction and Raman spectroscopic results. Furthermore, the optical spectroscopic results are provided as a supporting evidence for the existing band structural stability of the $Pb(NO_3)_2$ samples at shocked conditions.

2. Experimental section

The growth details of the title crystal have been discussed in the previous publication [16]. The details of the shock tube [35] and shock wave loading procedure are given in the supplementary section. In this experiment, the shock waves of Mach number 2.2 have been utilized which has the transient pressure 2.0 MPa and transient temperature 864 K. The sample has been well grained using a mortar such that three powder samples of equal quantity have been separated and among the three samples, one sample has been kept as the control sample and the rest have been utilized for the shock wave recovery experiment. Subsequently, 50 and 100 shock pulses of the same Mach number 2.2 have been applied to the samples and the respective samples have been put under XRD, Raman and DRS spectral analyses to understand the crystallographic structural stability of the $Pb(NO_3)_2$ samples. The analytical instruments details are as follows; Powder X-ray diffraction (PXRD) [Rigaku - SmartLab X-Ray Diffractometer, Japan- $CuK\alpha_1$ as the X-ray source ($\lambda = 1.5407$ Å), with the step precision of $\pm$ 0.001°], a Renishaw model Raman spectrometer with Laser line 532 nm and power 50 mW and an ultra-violet diffused reflectance spectroscope (UV-DRS-ShimadzuUV-3600 plus) have been utilized so as to understand the structural stability of the test samples at shocked conditions.

3. Results and discussion

3.1. X-ray diffraction studies

X-ray diffractometry has been performed to assess the crystallographic structural stability of the $Pb(NO_3)_2$ samples at dynamic shocked conditions and the recorded XRD pattern of the control and shocked lead nitrate samples are presented in Fig. 1a. For the conformation of phase purity, the comparison is made between the control sample and simulated XRD pattern (CIF: COD-5910007) such that both the XRD patterns are found to be well-matched with respect to the diffraction peak positions as well as intensity ratios of diffraction peaks. The diffraction peaks of the control sample are located at 19.630°, 22.701°, 25.426°, 27.837°, 32.313°, 38.052°, 39.802°, 46.258°, 50.763°, 52.197°, 57.506°, 61.408°, 67.405°, 71.078°, 72.139° and 76.750°, respectively and the obtained diffraction peak positions are finely corroborated with the cubic crystal structure with the *P*a-3 space group (CIF: COD – 5910007) [16]. Hence, it could be confirmed that the test sample has *P*a-3 space group symmetry such that the observed sharp diffraction peaks of the control sample clearly disclose the higher degree of crystalline nature.

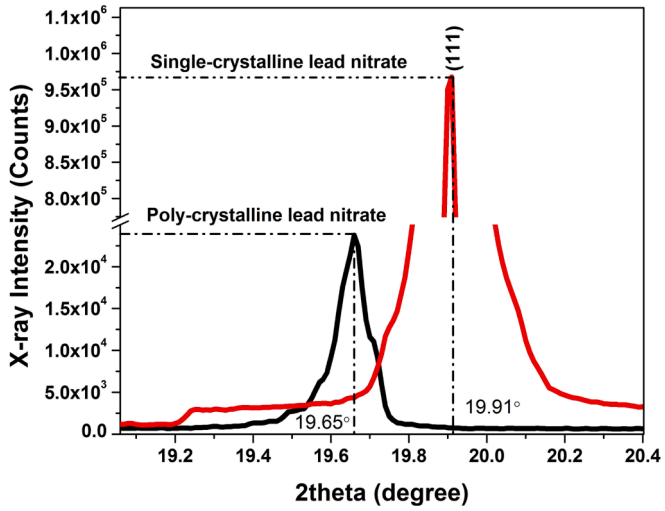

Fig. 2. Zoomed-in version of the (1 1 1) plane of the single and poly-crystalline $Pb(NO_3)_2$ samples.

Shocked samples' (50 and 100 shocked) XRD patterns are presented in Fig. 1 itself and as seen in Fig. 1a, the observed XRD patterns are almost similar to the control sample. Based on the initial assessment of the XRD patterns, it is clear that the test sample does not undergo any crystallographic phase transitions or amorphous phase transitions at shocked conditions like that of the single crystal of lead nitrate and the corresponding diffraction patterns are presented in Fig. 1b and the XRD patterns have been published previously [16].

Based on the observed X-ray diffraction results, it could be known that the poly-crystalline samples have higher crystallographic structural stability and shock resistance than that of the single crystalline materials and such results are found to be well-matched with the previous results of single and poly-crystalline materials [10,11,17,21]. Note that K_2SO_4 [10] and $CuSO_4{\cdot}5H_2O$ [15] single crystals undergo significant crystallographic phase transitions at shocked conditions and their respective poly-crystalline forms do not experience such structural phase transitions. In addition to that, in the case of single crystalline samples of K_2SO_4 [10] and $CuSO_4{\cdot}5H_2O$ [15] crystals, just a single shock pulse has induced significant structural changes. K_2SO_4 [10] undergoes polymorphic phase transition from β-α K_2SO_4 at the first shocked condition and in the case of $CuSO_4{\cdot}5H_2O$, crystalline state transforms to the amorphous state at the first shocked condition [15]. Moreover, lead nitrate single crystal experiences the dynamic re-orientational process from (1 1 1) to (6 0 0) at the first shocked condition whereas at the 3rd shocked condition, it undergoes a transition to the amorphous state [16]. But in the present case, even though the shock strength is increased to 100 times greater than that of the single crystal, no remarkable change has occurred. Hence, based on the overall observation, we could consider that the poly-crystalline sample has higher shock resistance than that of the single crystal of lead nitrate and such high shock resistance may be due to the formation of high-strained local grains and grain boundaries. As seen in Fig. 2, there are remarkable differences in the X-ray intensity of the plane (1 1 1) between the single crystalline and poly-crystalline samples which are quite common, because single crystals have highly ordered structure with preferred orientation along (1 1 1) such that single crystals always give rise to higher X-ray intensity.

While looking at the diffraction peak positions, the peak (1 1 1) of single crystalline lead nitrate is located at 19.91° whereas the peak (1 1 1) of poly-crystalline sample is located at 19.65° and the observed 0.25° lower angle shift in the poly-crystalline sample is due to the formation of strained crystal lattice [35–38]. Generally, poly-crystalline materials form higher lattice stress and strain than that of single crystals due to the higher density grain boundaries and higher lattice deformations [17,31–33]. Such grain boundary interfaces actually provide high resistance to external forces such as temperature, pressure etc so that these materials are capable enough to withstand the elastic and plastic deformations induced by the external stimuli. Note that local grains in the polycrystalline matrix always try to maintain the original yield state during the encounter with external parameters such as temperature, pressure and forces that typically induce deformation. Therefore, the grain boundary interfaces in polycrystalline materials could resist the external forces more than that of single crystals. In addition to that, if the deformation process has to be started by the above-mentioned external parameters, it should start from a single slip or single plane system which has to transform gradually into multiple slip systems because of the orientational evolution in poly-crystals that are quite complex in comparison to the single crystals and hence the stress and strain compatibility in-between grains is much higher in poly-crystals. Hence, in the case of poly-crystalline samples, higher shock

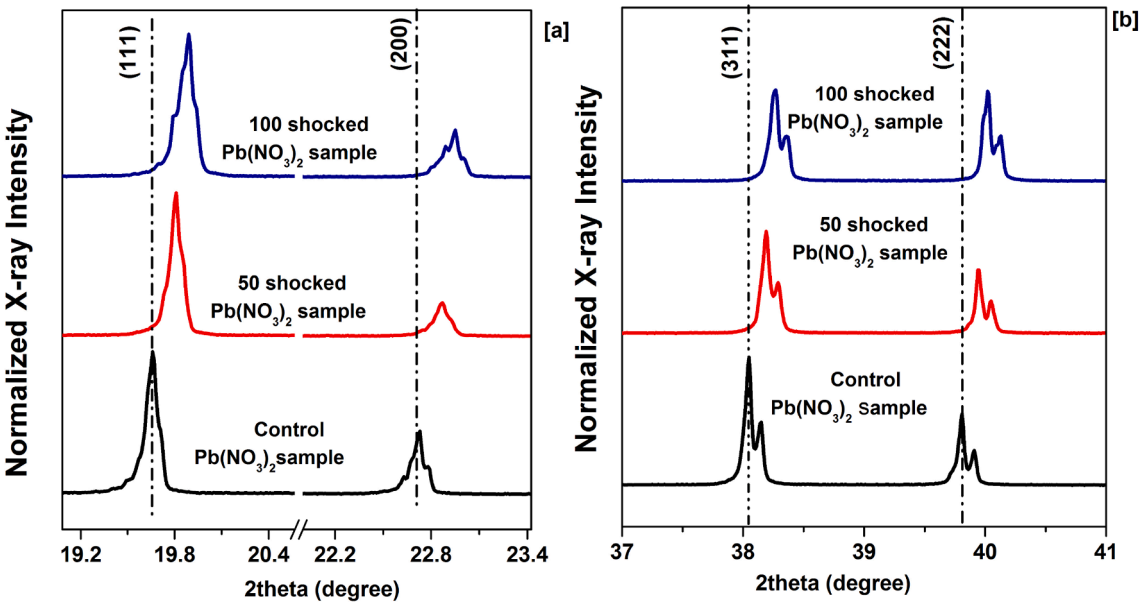

Fig. 3. Zoomed-in versions of the crystalline plane profiles of the control and shocked poly-crystalline $Pb(NO_3)_2$ samples.

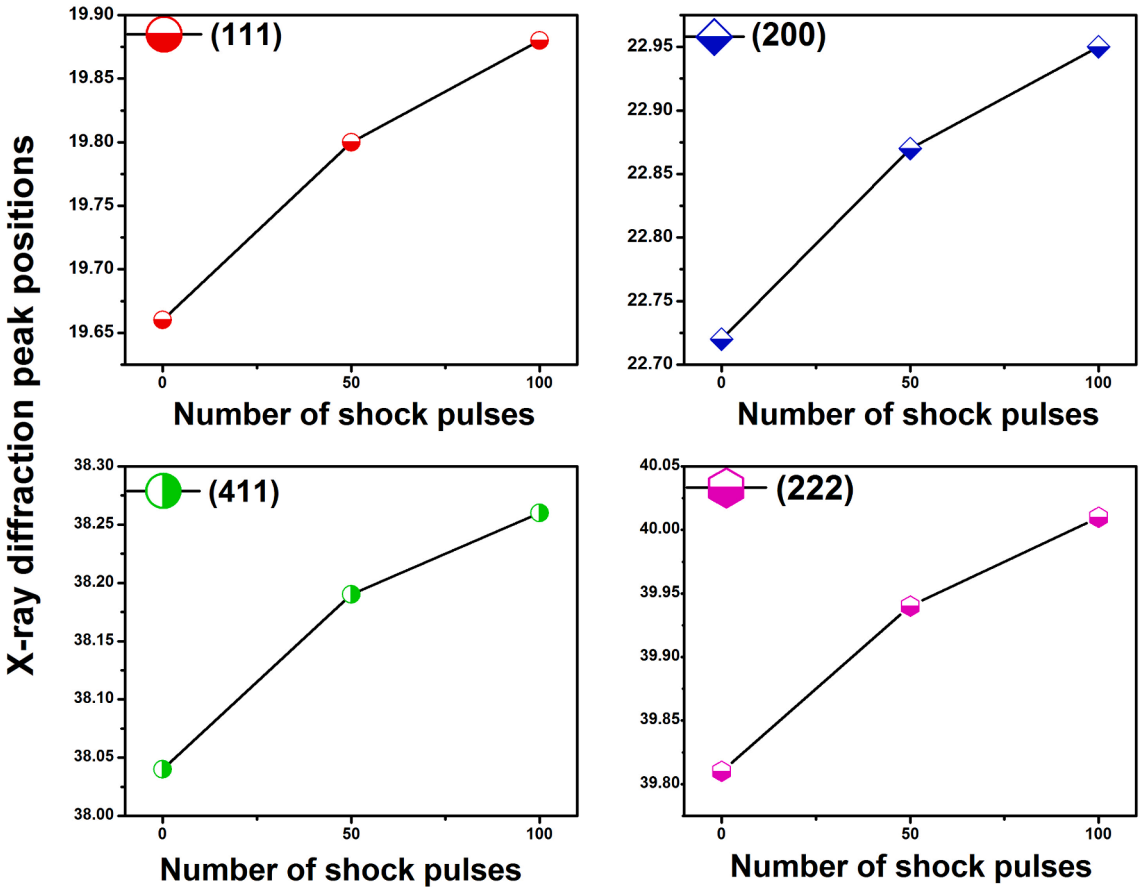

Fig. 4. Diffraction peak shifts of the $Pb(NO_3)_2$ samples with respect to the number of shock pulses.

pressure is required to induce the transformations and lattice deformations as compared to single crystals [31–33]. Moreover, generally during the shocked conditions, single crystals are prone to undergo rotational order and disorder process as in the case of sulfate (SO_4) [10] and nitrate (NO_3) anionic systems [16] because of the less lattice strain and the rotational disorder. But in the present case, due to the higher density of grain boundary, the NO_3 units donot undergo the rotational disorder at shocked conditions and hence the title sample retains its original crystal structure. To get a deeper understanding of the structural stability of the poly-crystalline $Pb(NO_3)_2$ samples at shocked conditions, we have presented the zoomed-in versions of the different crystalline planes such as (111), (200), (311) and (222) in Fig. 3. As seen in Fig. 3a and Fig. 3b, the diffraction lines have shifted towards the higher angle with respect to the number of shock pulses which may be due to the lattice compression during the shocked conditions [12].

At shocked conditions, none of the crystalline peak has disappeared and no new diffraction peak has appeared as reflected in Fig. 1 of Pb $(NO_3)_2$ samples. Note that, in the case of magnesium bromide micro-sized poly-crystalline samples [22], new diffraction lines have appeared at shocked conditions due to the shock wave induced micro distortions and lattice deformations. Similarly, in the case of the potassium dihydrogen phosphate [19], glycine phosphite [20] poly-crystalline samples, a couple of diffraction peaks disappear at 50 shocked conditions and reappear at 100 shocked conditions. But, in the present case, there is no such change noticed and hence it is clear that the applied shock waves do not induce any significant lattice deformations. In addition to that, as seen in Fig. 3, the intensity ratio of diffraction peaks is slightly changed with respect to the number of shock

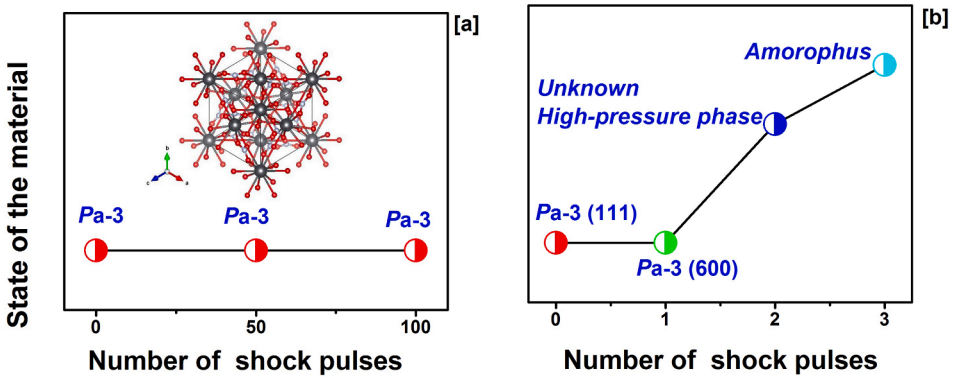

Fig. 5. Shock- phase profiles of $Pb(NO_3)_2$ samples (a) poly-crystal (b) single crystal.

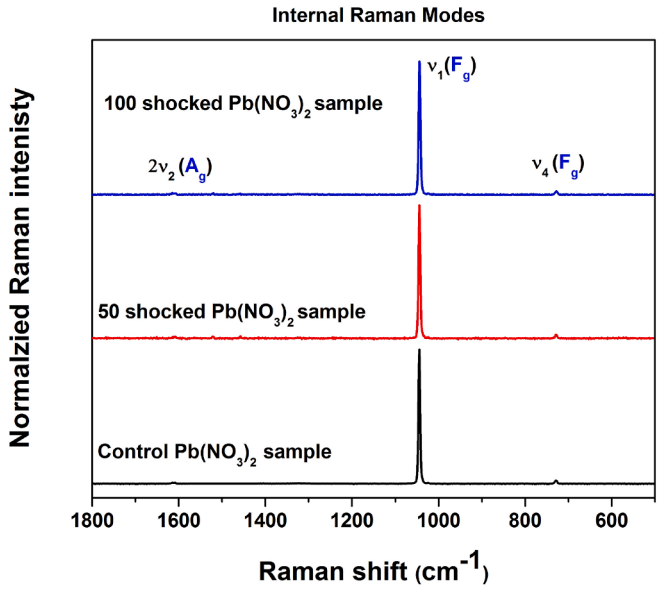

Fig. 6. Internal Raman modes of the control and shocked $Pb(NO_3)_2$ samples.

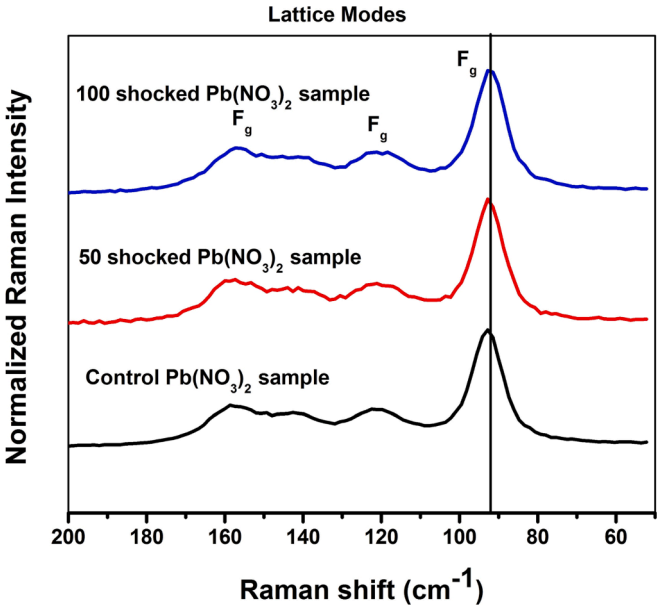

Fig. 7. Lattice Raman bands for the control and shocked $Pb(NO_3)_2$ samples.

pulses and such changes are not controllable in the poly-crystalline state materials. Fig. 4 shows the (111), (200), (411) and (222) planes that suffer a marginal shift with respect to the number of shock pulses and based on the observed profiles, while increasing the number of shock pulses, the diffraction lines are shifted towards the higher angle side which discloses the occurrence of lattice compression with respect to the number of shock pulses. During the shocked conditions, the intra-bond length might have reduced resulting in the lattice compression.

Furthermore, based on the observed diffraction results of the single and poly-crystalline samples at shocked conditions, the shocked phase profiles are made for the single and poly-crystalline samples as presented in Fig. 5.

3.2. Raman spectroscopic results

In order to obtain further reinforcement on the structural stability of the poly-crystalline samples at dynamic shocked conditions, the Raman spectral analysis has been carried out for the control and shocked samples. Referring to the results of the shock wave recovery experiment on the single crystal lead nitrate, significant changes have occurred in Raman bands [39,40]. Hence, Raman spectral investigations could provide additional authentic confirmation on the stability of the test samples' crystallographic structure at shocked conditions such that the Raman measurement has been performed over the wave-number region between 50 and 2000 cm^{-1} and the obtained internal and external Raman bands of the control and shocked samples are presented in Fig. 6 and Fig. 7. As seen in Fig. 6, Raman spectrum of the control sample has three Raman bands that are located at 730 (F_g), 1043 (F_g), 1612 cm^{-1} (A_g), respectively and the observed Raman bands are found to be well-matched with the previously reported *P*a-3 symmetry lead nitrate [15]. Among the three Raman bands, 1043 cm^{-1}(F_g) mode has a dominant Raman peak intensity that is not altered so also the Raman band location at shocked conditions. Moreover, all the Raman bands (F_g and A_g polarization modes) retain their original intensity as well as Raman band locations. Hence, based on the observed Raman bands profiles with respect to the number of shock pulses, the test sample is identified to have not undergone any kind of structural phase transitions from crystalline to crystalline state or crystalline to amorphous state even as high as 100 shocked conditions.

Note that, in the case of the single crystal experiment, $2\upsilon_2$ (A_g) Raman mode has completely disappeared at the 3rd shocked condition and υ_1 (F_g) shoulder Raman mode has also disappeared at shocked conditions and such signatures are the possible reasons for the amorphous state at the 3rd shocked condition. But, in the present case, such changes could not be observed even at the 100 shocked conditions. Hence, it could be confirmed that the poly-crystalline state sample has high shock resistance than that of the single–crystalline lead nitrate. Such kind of high shock resistant materials can be better prospects for the industrial applications [41–43]. Furthermore, the lattice mode Raman bands of the control and shocked $Pb(NO_3)_2$ samples are shown in Fig. 7 such that the lattice mode of the Raman bands also reflects a similar conclusion on the structural stability of the $Pb(NO_3)_2$ sample at dynamic shock exposed conditions. Note that, according to the group theory, a particular crystal lattice symmetry has its own external Raman bands and if there is any kind of crystallographic phase transition occurs, either the external Raman bands are altered in terms of Raman shift or new lattice Raman bands appear/ disappear according to the new crystallographic phase formed [16]. In the present case, the external Raman bands are found at 93, 121, and 158 cm^{-1} and the observed lattice Raman band locations are well-matched with the previous reports [39,40]. Lattice Raman mode intensity is also one of the important parameters with which the phase stability can be understood such that, if there is any deformation, it could be identified. Hence, the Raman band intensity is considered as one of the major points of discussion on the structural stability of the test sample at shocked conditions. Moreover, it gives quantitative information on the number of disorders experienced by the title material at shocked conditions. At shocked conditions, there is no change found in the Raman peak positions and neither a new peak appears nor the existing peaks disappear. Hence, it confirms that the test sample has a stable crystallographic structure at shocked conditions.

3.3. Optical properties

Note that, in the case of single crystals such as K_2SO_4 [10], sodium sulfate [11], ADP [12], KDP [13], and $PbNO_3$ [16], lots of changes have been found in their respective optical transmittance and optical absorption edges with respect to the number of shock pulses because of the formation of lattice deformations and structural phase transitions. Hence, the optical spectroscopic results are very much required to make a crystal clear conclusion on the stability of the crystal structures and hence the optical transmittance spectra have been measured over the wavelength region between 200 and 800 nm for the control and shocked

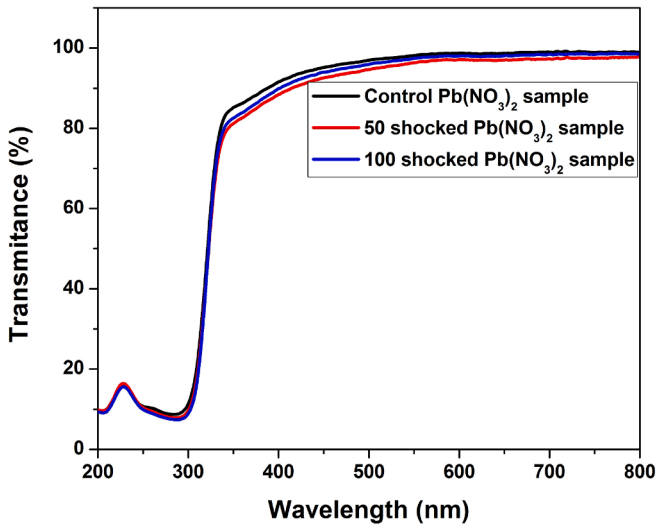

Fig. 8. Optical transmittance spectra for the control and shocked Pb $(NO_3)_2$ samples.

samples using a UV-DRS- Shimadzu- UV-3600 plus spectrometer and the profiles of the obtained optical transmittance are presented in Fig. 8.

As seen in Fig. 8, the primary nitrate ion's absorption band appears between 200 and 250 nm [16] such that the absorption edge positions as well as their initial band shape are not altered at shocked conditions. It could be noted that the poly-crystalline ADP [18] and KDP samples [19], suffer significant absorption band shifts with respect to the number of shock pulses and such absorption band shifts occur due to the changes in the degree of crystalline nature. But, in the present case, no change is observed either in the optical transmittance or in the absorption band shifts such that it is one of the alternative proofs to justify the electronic band structural stability in the poly-crystalline lead nitrate samples at shocked conditions.

4. Conclusion

On consolidating the obtained experimental findings, we have investigated the structural stability of the single and poly-crystalline lead nitrate samples at shocked conditions such that the shock resistance has been analyzed by the X-ray diffraction and Raman spectroscopic techniques and the observed optical spectroscopic results could provide the solid authentication. X-ray diffraction results show that all the diffraction peaks are retained at shocked conditions i.e. none of the peak disappears and no new peak appears. The obtained slight higher angle shift in the XRD patterns may be due to the unit cell compression with respect to the number of shock pulses. Raman spectral results clearly disclose the stability of the internal and external Raman modes at shocked conditions and the optical spectroscopic results also agree well with the XRD and Raman spectral results on the shock resistance of the test samples. As per the observed results of the analytical techniques, it is clear that the poly-crystalline lead nitrate samples have a high-shock resistance compared to the single crystalline samples. Hence, based on the observations, it is proposed that the poly-crystalline lead nitrate could be utilized for device-based applications. This kind of comparison of single and poly-crystalline materials at shocked conditions can provide a road map for a better understanding of the properties of materials at shocked conditions with respect to the control state.

CRediT authorship contribution statement

A. Sivakumar: Conceptualization, Methodology, Writing – original draft. **P. Eniya:** Methodology, Software. **S. Sahaya Jude Dhas:** Writing – review & editing. **Lidong Dai:** Conceptualization. **P. Sivaprakash:** Formal analysis. **Raju Suresh Kumar:** Formal analysis. **Abdulrahman I. Almansour:** Formal analysis. **J. Kalyana Sundar:** Formal analysis. **Ikhyun Kim:** Formal analysis. **S.A. Martin Britto Dhas:** Supervision.

Declaration of Competing Interest

The authors declare that they have no known competing financial interests or personal relationships that could have appeared to influence the work reported in this paper.

Data availability

Data will be made available on request.

Acknowledgment

The authors thank NSF of China (42072055). The project was supported by Researchers Supporting Project number (RSP2023R142), King Saud University, Riyadh, Saudi Arabia.

Appendix A. Supplementary data

Supplementary data to this article can be found online at https://doi.org/10.1016/j.mseb.2023.116839.

References

[1] X. Zhou, Y.-R. Miao, W.L. Shaw, K.S. Suslick, D.D. Dlott, J. Am. Chem. Soc. 141 (2019) 2220–2223.
[2] Nagarajan Kirupakaran Gopinath, Gopalan Jagadeesh, Bikramjit Basu, J Am Ceram Soc. 00 (2019) 1–14.
[3] S.u. Zhi, W.L. Shaw, Y.-R. Miao, S. You, D.D. Dlott, K.S. Suslick, J. Am. Chem. Soc. 139 (2017) 4619–4622.
[4] T. de Rességuier, O.O. Kurakevych, A. Chabot, J.P. Petitet, V.L. Solozhenko, J. Appl.Phys 108 (2010), 083522.
[5] D.E. Hooks, K.J. Ramos, A. Richard Martinez, J. Appl.Phys 100 (2006), 024908.
[6] P. A. Urtiew; J.Appl.Phys 45 (1974) 3490.
[7] Z.A. Dreger, Y.A. Gruzdkov, Y.M. Gupta, J.J. Dick, J. Phys. Chem. B 106 (2002) 247–256.
[8] E. Lin, H. Shi, L. Niu, M. Simul, Mater. Sci. Eng. 22 (2014), 035012.
[9] K. Ichiyanagi, S.-I. Adachi, S. Nozawa, Y. Hironaka, K.G. Nakamura, T. Sato, A. Tomita, S.-Y. Koshihara, Appl. Phys. Lett. 91 (2007), 231918.
[10] A. Sivakumar, S. Reena Devi, S. Sahaya Jude Dhas, R. Mohan Kumar, K. Kamala Bharathi, S.A. Martin Britto Dhas, Cryst. Growth Des. 20 (2020) 7111–7119.
[11] A. Sivakumar, S. Sahaya Jude Dhas, P. Sivaprakash, Abdulrahman I. Almansour, Raju Suresh Kumar, Natarajan Arumugam, S. Arumugam, S. A. Martin Britto Dhas, New J. Chem. 45 (2021) 16529.
[12] A.Sivakumar, S. Sahaya Jude Dhas, S.Balachandar, S.A. Martin Britto Dhas, Z. Kristallogr. 234 (2019) 557–567.
[13] A. Sivakumar, M. Manivannan, S. Sahaya Jude Dhas, J. Kalyana Sundar, M. Jose, S. A. Martin Britto Dhas, Mater. Res. Express 6 (2019), 086303.
[14] A. Sivakumar, S. Reena Devi, J. Thirupathy, R. Mohan kumar, S.A. Martin Britto Dhas, J. Elect.Mater 48 (2019) 7216–7225.
[15] A. Sivakumar, S. Sahaya Jude Dhas, Abdulrahman I. Almansour, Raju Suresh Kumar, Natarajan Arumugam, S. A. Martin Britto Dhas, Cryst. Eng. Comm. 23 (2021) 7044.
[16] A. Sivakumar, P. Eniya, S. Sahaya Jude Dhas, Raju Suresh Kumar, Abdulrahman I. Almansour, Kundan Sivashanmugan, J. Kalyana Sundar, S.A. Martin Britto Dhas, Cryst. Engg. Comm. 24 (2021) 52-56.
[17] A. Sivakumar, S. Sahaya Jude Dhas, Abdulrahman I. Almansour, Raju Suresh Kumar, Natarajan Arumugam, Karthikeyan Perumal, S.A. Martin Britto Dhas, Solid State Commun 340 (2021) 114508.
[18] A. Sivakumar, A. Saranraj, S. Sahaya Jude Dhas, K. Showrilu, S.A. Martin Britto Dhas, Z. Kristallogr 236 (2021) 1–10.
[19] A. Sivakumar, S. Sahaya Jude Dhas, S. Balachandar, S.A. Martin Britto Dhas, J. Elect. Mater 48 (2019) 7868–7873.
[20] A. Sivakumar, S. Sahaya Jude Dhas, S.A. Martin Britto Dhas, Solid State Sci. 110 (2020), 106452.
[21] A. Sivakumar, S. Sahaya Jude Dhas, J. Elberin Mary Theras, M. Jose, P. Sivaprakash, S. Arumugam, S.A. Martin Britto Dhas, Solid State Sci. 121 (2021) 106751.
[22] A.N. Zhukov, N.S. Sidorov, A.V. Palnichenko, V.V. Avdonin, D.V. Shakhraia, High. Press. Res. 29 (2009) 414–421.
[23] A. Sivakumar, A. Saranraj, S. Sahaya Jude Dhas, P. Sivaprakash, S. Arumugam, S.A. Martin Britto Dhas, Spectrochim. Acta Part A. 242 (2020) 118725.
[24] S. Kalaiarasi, A. Sivakumar, S.A. Martin Britto Dhas, M. Jose, Mater. Lett. 219 (2018) 72–75.
[25] V. Jayaram, K.P.J. Reddy, Adv. Mater. Lett. 7 (2016) 100–150.

[26] A. Sivakumar, S. Soundarya, S. Sahaya Jude Dhas, K. Kamala Bharathi, S. A. Martin Britto Dhas, J. Phys. Chem. C. 124 (2020) 10755−10763.
[27] M. Devika, N. Koteeswara Reddy, V. Jayaram, K.P.J. Reddy, Adv. Mater. Lett. 8 (2017) 398–403.
[28] A. Rita, A. Sivakumar, S.A. Martin Britto Dhas, J. Supercond. Nov. Magn. 33 (2020) 1845–1849.
[29] V. Jayarama, K.P.J. Asha Gupta, J. Reddy, Adv. Ceram. 3 (2014) 297–305.
[30] K. Vasu, H.S.S.R. Matte, S.N. Shirodkar, V. Jayaram, K.P.J. Reddy, U.V. Waghmare, C.N.R. Rao, Chem. Phys. Lett. 582 (2013) 105–109.
[31] G. Franz, F. Abed-Meraim, M. Berveiller, Int. J. Plast 48 (2013) 1–33.
[32] M. Hafok, R. Pippan, Mater. Sci. Forum 550 (2007) 277–282.
[33] G. Das, Cer. Eng. Sci. Proc. 16 (2008) 977–986.
[34] L. Mezeix, D.J. Green, Int. J. Appl. Ceram. Technol. 3 (2006) 166–176.
[35] A. Sivakumar, S. Balachandar, S. A. Martin Britto Dhas, Hum. Fact. Mech. Eng. Defense. Safety. 4 (2020) 3.
[36] X. Li, C. Chen, H. Deng, H. Zhang, D.i. Lin, X. Zhao, H. Luo, Crystals 5 (2015) 172–192.
[37] C. Elschner, M. Schrader, R. Fitzner, A.A. Levin, P. Buerle, D. Andrienko, K. Leo, M. Riede, RSC Adv. 3 (2013) 12117.
[38] R.Weber Fell C.R., J.R. Dahn, S. Hy, J. Electrochem. Soc. 164 (2017) 2992–2999.
[39] M.H. Brooker, J. Solid State Chem. 28 (1979) 29–39.
[40] H. Isoda, A. Sakai, R. Kawashima, J. Phys. Soc. Japan. 76 (2007), 065001.
[41] K. Manimekalai, P. Jayaprakash, J. Mater. Sci. Mater. Electron. 32 (2021) 8033–8042.
[42] E. Raju, P. Jayaprakash, G. Vinitha, N. Saradha Devi, S. Kumaresan, J. Mater. Sci. Mater. Electron. 32 (2021) 21155–21163.
[43] A. Sivakumar, S. Sahaya Jude Dhas, Raju Suresh Kumar, Abdulrahman I. Almansour, Magesh Murugesan, S. A. Martin Britto Dhas, Phys. Status Solidi B (2022) 2100540.